Liquid metal-tailored gluten network for protein-based e-skin

Bin Chen
Fudan University
Yudong Cao
Fudan University
Zhuo Yan
Fudan University
Rui Liu
Tianjin University of Science & Technology
Yunjiao Zhao
Tianjin University of Science & Technology
Xiang Zhang
Rice University https://orcid.org/0000-0003-4004-5185
Minying Wu
Fudan University
Yixiu Qin
Fudan
Chang Sun
Fudan University
Wei Yao
Fudan University
Ziyi Cao
Fudan University
Pulickel Ajayan
Rice University https://orcid.org/0000-0001-8323-7860
Mason Chee
George Mason University
Pei Dong
Department of Mechanical Engineering, George Mason University, Virginia
Zhaofen Li
RENISHAW (SHANGHAI) TRADING CO.LTD
Jianfeng Shen
Institute of special materials and technology, Fudan University
Mingxin Ye (mxye@fudan.edu.cn)

Fudan University

Article

Keywords: Gluten, Protein, EGaIn, Electronic skin, Biocompatibility

Posted Date: August 6th, 2021

DOI: https://doi.org/10.21203/rs.3.rs-233836/v1

Version of Record: A version of this preprint was published at Nature Communications on March 8th, 2022. See the published version at https://doi.org/10.1038/s41467-022-28901-9.

Abstract

Designing electronic skin (e-skin) with proteins is a critical way to endow e-skin with biocompatibility, but engineering protein structures to achieve controllable mechanical properties and self-healing ability remains a challenge. Here, we develop a hybrid gluten network through the incorporation of an eutectic gallium indium alloy (EGaIn) to design a self-healable e-skin with improved mechanical properties. The intrinsic reversible disulfide bonds/sulfhydryl groups reconfiguration of gluten networks is explored as a driving mechanism to introduce EGaIn as chemical cross-linkers to create hierarchical sulphur bonds, thus inducing the secondary structure rearrangement of gluten to form additional β-sheets as physical cross-linkers. Remarkably, this strategy allows the gluten network to realize a synthetic material-like stretchability (>1600%) and to endure a three-dimensional strain change. The obtained e-skin is biocompatible and biodegradable, and can sense strain changes from different scale human motions. The protein network micro-regulation method paves the way for future skin-like protein-based e-skin.

Introduction

The increasing demand of electronic skin (e-skin) in the fields of skin attachable devices, robotics and prosthetics has motivated various cutting-edge technologies to endow e-skin with skin-like sensory capabilities and outstanding mechanical properties, but unfortunately e-skin with biocompatibility presents great challenges for practical on-skin applications[1-3]. Therefore, despite the current existence of different kinds of reported synthetic materials, there is still a strong desire for exploring biocompatible e-skin materials. Given that protein is a vital component of skin, proteins are the ideal option to provide biocompatibility for e-skin[4]. However, designing e-skin with proteins is still in its infancy, because precisely controlling the microstructure of proteins to obtain adjustable mechanical properties and self-healing abilities is fairly complicated.

Silk fibroin (SF), the dominant protein in e-skin research, has demonstrated feasibility for fabricating e-skins with tunable mechanical behaviors and biocompatibility through complex plasticizing or carbonizing pretreatments[4-8]. In this regard, the gluten protein is proposed for preparing e-skin by a simple method. Upon hydration and kneading, gluten is known to form a cross-linked three-dimensional protein polymeric network through intra- and inter-molecular covalent and noncovalent bonds. The gluten network possesses various dynamic bonds, like dynamic covalent disulfide (S-S) bonds and noncovalent H-bonds, thus guaranteeing the self-healing ability that most SF-based e-skin loses[1, 9-12]. Generally, for e-skin preparation, the macroscopic mechanical performances of synthetic materials, like supramolecular polymers, can be adjusted by constructing cross-linking positions inside the microscopic network structure[13-15]. However, strengthening and toughening the soft gluten network by achieving the co-incorporation of physical and chemical cross-linking sites at the molecular level remains a challenge. Fabricating a gluten-based e-skin through network regulation would lead to a more sophisticated control over mechanical properties and self-healing ability.

To address this issue, on the hypothesis that the abundant free sulfhydryl (-SH) groups of gluten may provide reactive sites to construct dynamic cross-linking bonds in a metal-ligand interactive form, the eutectic gallium indium alloy (EGaIn) that thiolate ligands favorably react with is introduced to improve the gluten network[16, 17]. Therefore, this structural characteristic is explored to design an EGaIn/gluten-based e-skin (E-GES) in this work. Our strategy targets the reversible -SH/S-S exchange mechanism in gluten network to introduce EGaIn as chemical cross-linkers and thus establish hierarchical S-bonds in E-GES networks in which S-S bonds maintain the structural integrity, while EGaIn-SH coordinative bonds contribute to dissipating energies. Surprisingly, the rearrangement of gluten protein chains causes an increase in β-sheets which act as physical cross-linking points[18, 19]. Thus, the high-density cross-linking sites and various dynamic bonds endow E-GES with exceptional mechanical strength and toughness respectively. Furthermore, E-GES can withstand the spatial strain variation, behaving like conventional rubber materials. Such characteristics make E-GES a competitive strain sensor for sensing strain signals from different human motions. In summary, through the dynamic network micro-regulation mechanism of gluten networks, we realize the combination of liquid metal and protein to achieve a protein-based e-skin, which could provide insights on metal-protein interactive mechanics to develop more proteins for e-skin.

Main Text

Gluten network regulation by EGaIn

Gluten extracted from wheat flour is a mixture of polymeric glutenins and monomeric gliadins subunits[20]. In the hydration and kneading process, glutenins tend to align and form a cross-linked three-dimensional gluten protein polymeric network through intra- and inter-molecular S-S bonds and noncovalent bonds thus contributing to the strength and elasticity, while gliadins combine with the formed glutenin structures by non-covalent bonds and influence the viscous properties of the protein matrix[21]. It is worth noting that, to produce a stronger protein network, a small amount of salt is needed during this process, because the net positive charge of gluten can be shielded by salt, thus decreasing the electrostatic repulsion between gluten molecules and making them combine closely[22, 23]. Different from the wheat dough, there are no starch granules embedded in the framework of the E-GES network. As shown in Fig. 1a, E-GES was prepared by mixing the gluten with EGaIn-dispersed solutions with the addition of a small amount of NaCl and kneading. According to the mass ratio of EGaIn in gluten, the obtained E-GES samples are named as 1%, 3%, 5% and 10% respectively, with the sample without EGaIn addition as control denoted as 0%. The formation of different secondary structures of E-GES are revealed by analyzing the amide I absorption bands on Fourier transform infrared spectroscopy (FTIR) (discussed later) (Supplementary Fig. 1). The typical peak appearing at 521 cm^{-1} in the Raman spectra confirms the formation of S-S bonds in E-GES, representing the trans-gauche-gauche conformations of S–S bonds, and the peak at around 2478 cm^{-1} indicates the presence of -SH bonds (Supplementary Fig. 2)[24, 25]. Furthermore, it has been demonstrated that thiolated ligands are readily attached to the interface of EGaIn[16], so the abundant -SH groups of gluten are expected to provide reactive sites to EGaIn. This

expectation is confirmed by the distinct binding energy shift of S 2p region observed in X-ray photoelectron spectroscopy (XPS) along with the redistribution of -SH/S-S contents in response to higher EGaIn concentration (Fig. 1b,c)[26]. The increasing trend of free -SH content, released from the combination with EGaIn during analytical test, reinforces this standpoint. Importantly, Fig. 1d-g show that E-GES has a more regular and denser structure than that of the control sample, meaning that the decrease in the S-S content does not influence the structural integrity of the gluten network, and the energy-dispersive X-ray spectroscopy (EDS) mapping result reveals the presence of EGaIn. Therefore, the EGaIn has been successfully introduced into the gluten network through the construction of intermolecular EGaIn-SH coordinative bonds, and contributes to the adjustment of the gluten network in turn. The obtained E-GES can be stretched easily by hands (Fig. 1h), and molded to entirely different shapes (Fig. 1i), suggesting its ability to adhere well to irregular body surfaces.

Connections between macroscopic behaviors and microscopic structures of E-GES

To qualify for e-skin preparation, we first introduce EGaIn to tailor the microscopic structure of gluten, thus improving its macroscopic mechanical properties. The designed E-GES are considerably strengthened and toughened as reflected in the increased tensile strength, tensile toughness as well as stiffness shown in Fig. 2a. The increase in the content of EGaIn contributes to improved mechanical performance with the maximum tensile stress, dissipated energy and Young's modulus increasing from 13.5 kPa, 228.2 KJ/m^3 and 11.9 kPa to 51.2 kPa, 597.1 KJ/m^3 and 25.2 kPa respectively when EGaIn content is 5% (Supplementary Fig. 3). By contrast, the breaking strain exhibits a decreasing trend and shows a minimum value of around 1600%. However, human skin generally suffers from around 30% of the tensile strain in daily human motions, and some reports suggest that the skin-like wearable flexible hybrid electronics with stretchability as high as 100% are in favor of obtaining high-quality signals from skin[1, 27]. Thus, the trade-off of the tensile strain of E-GES is acceptable and quite normal, and its remaining stretchability is comparable with that of many synthetic materials, a rarely reported phenomenon for protein-based material in previous studies (Fig. 2c)[13, 15, 28-31]. Insights into the microscopic structure of E-GES are obtained through FTIR analysis. The changes of the gluten backbone conformation are revealed by analyzing amide I bands (1700-1600 cm^{-1}) as illustrated in Fig. 2d, e and Supplementary Fig. 4. The high content of α-helix in all E-GES samples suggests they have more ordered gluten network structure compared with other gluten modification jobs (around 20% to 30% of α-helices) (Supplementary Fig. 5)[9, 10]. The incorporation of EGaIn facilitates the formation of a higher proportion of β-sheets, the most stable conformation of gluten, at the expense of α-helix in a dose-dependent manner. This result is likely attributed to the reduction of intermolecular S-S bonds and the changes of interactions among intramolecular H-bonds induced by EGaIn[9]. It is worthwhile to note that these nanocrystals-like β-sheets can act as many physical crosslinking points embedded in the amorphous protein network, thus defining the mechanical properties of protein, as widely received in the studies for silk protein[18, 32]. The cross-linked gluten protein chains clearly show restricted chain mobility as exposed by differential scanning calorimetry (DSC) (Fig. 2f). The enhancing thermal stability declares the raise in crystallinity and the order of E-GES network structure by denaturation temperature value changing from

48.26 °C to 58.17 °C under different EGaIn dosages (Supplementary Table 1). This is consistent with the current understanding about the influence of cross-linking degree and crystallinity toward the glass-transition temperature of polymer, and the study of graphene oxide/SF composite materials[19]. Moreover, except for the β-sheet physical cross-linking sites, there are abundant chemical cross-linking points because of the coordinative interactions between EGaIn and the -SH groups of gluten, so a large number of high-density cross-linking sites synergistically promote the adjustment of the E-GES network structure. On the other hand, the changes in the E-GES networks also can be observed from the variation of their viscoelasticity. The rheological characterizations show that all samples display a solid-like behavior with a storage modulus (G') greater than the loss modulus (G"), and E-GES samples have increased their G' and G" by one to two times compared with the control sample (Fig. 2g and Supplementary Fig. 6). The improving viscoelasticity of E-GES agrees well with its enhanced mechanical performance in tensile test results. These outcomes indicate that we successfully create a hybrid cross-linking gluten network in E-GES through the construction of additional coordinative bonds by EGaIn and the conformation transition to β-sheet by H-bonds rearrangement[14, 33]. In general, the improvement in the macroscopic strength and toughness of E-GES can be explained by the microscopic structural adjustment according to the proposed mechanism below: The presence of two different cross-linkers endowing E-GES with various dynamic chemical bonds lead to highly folded gluten protein chains, thus developing a hierarchical network structure, which is beneficial for withstanding tensile changes and dissipating energy (Fig. 2h). This mechanism is further corroborated by the growth in Young's modulus and dissipated energy with the increase of tensile strain rates (Fig. 2b), and the gradually growing internal fracture of E-GES network in the loading-unloading cycle tests with varying maximum strains (Supplementary Fig. 7), demonstrating the stiff and tough E-GES network structure. Besides, the robust E-GES network can withstand the three-dimensional spatial strain variation, which is easily visualized through a simple and intuitive mechanical experiment as shown in Fig. 2i. The membrane-shaped E-GES can be inflated into a balloon with a size range several orders of magnitude larger size range than before, which is an amazing phenomenon for protein-based materials or those hydrogel-like materials.

Self-healing ability and biocompatibility of E-GES

It is widely acknowledged that when wheat dough being teared, dough fragments can be rolled up and kneaded, thus making a reshaped dough without obvious performance degradation[11]. The principle behind it is the dynamic construction of and conversion between S-S bonds and free -SH groups together with the assistance of intramolecular and intermolecular H-bonds involved in the gluten network rebuilding process. Naturally, this intrinsic characteristic endows gluten networks with remarkable self-healing ability for making e-skin. The self-healing efficiencies of E-GES are evaluated through the following two aspects: stiffness recovery (Young's modulus-based) and toughness recovery (dissipated energy-based). The stress-strain curves demonstrate the healed E-GES recovers 97.9% of stiffness and 51.4% of its toughness after being cured from complete cutting (Fig. 3a). In order to examine the ultimate self-healing property of E-GES during the tensile experiment, we just simply put two cut-off E-GES pieces together for 1 min without any further treating, thus causing a circular wound on the healed E-GES under

this seriously restricted healing condition. This visible defect results in a local stress concentration, which is the main reason why the toughness decreases. However, the remaining stretchability was still measured to be up to 700% along with an almost unchanged Young's modulus, suggesting the exceptional self-healing ability of the strong E-GES network. The inherent self-healing mechanism of E-GES is deeply revealed by analyzing the change of the tyrosine (Tyr) side-chain mode of gluten as illustrated in the Raman spectra (Fig. 3b), because the variation of the intensity ratio between the Tyr doublet (I_{861}/I_{837}) provides H-bonding information of Tyr residues[24, 34]. The increase in the ratio valve indicates that Tyr residues tend to be exposed to a hydrophilic environment and possess the ability to form strong hydrogen bonds serving as proton acceptors. The ratio value changing from 1.17 to 1.65 shows that the combination of EGaIn promotes the Tyr residues exposure (Supplementary Fig. 8)[35]. Hence, the self-healing mechanism of E-GES can be summarized as follows: The presence of Tyr residues and EGaIn contributes to the formation of abundant H-bonds and coordinative bonds respectively in the cut interface, thus benefiting the initial recovery of E-GES network, and then the dynamic disulfide exchange between free -SH groups and S-S bonds accelerates the eventual recovery of E-GES network by covalent bonds (Fig. 3c), somewhat like the healing mechanism of thioctic acid-based supramolecular polymers[14]. Furthermore, the excellent self-healing ability of E-GES is also reflected in the conductivity recovery with an LED bulb lighting with slight contact between two cut interfaces (Fig. 3d). Intriguingly, we find that ultra-low temperatures cannot cause irreversible damage to E-GES, because it can recover the mechanical and conductive properties in a great measure as the temperature rises (Fig. 3e and Supplementary Fig. 9).

Apart from the necessary stretchability and self-healing ability, a qualified e-skin should be biocompatible. We specifically designed different experiments to estimate the effect of E-GES on the rabbit skin as shown in Fig. 3f, g. As for the skin with an artificial #-shaped wound, the attachment of E-GES does not affect the wound healing, and newborn rabbit hair can be observed on the wound after seven-day attachment experiments, similar to the result of the control wound without any treatments (Supplementary Fig. 10). In addition, there were no adverse reactions observed on the surrounding healthy skin. Given that e-skin inevitably reacts with sweat in daily use, whether the sweat will be polluted by e-skin and influence the health of skin is another important problem. With this in mind, E-GES was totally immersed into artificial sweat for 24 hours, and the treated sweat was applied to the healthy skin and the skin with the #-shaped wound respectively (Fig. 3g and Supplementary Fig. 11). Observation of the skin over a seven-day period definitively proves the excellent safety of E-GES when in contact with sweat. To protect the environment, we believe an attractive biocompatible e-skin candidate should also be biodegradable. The disappearance of E-GES in the pepsin solution and the appearance of mold on the surface of E-GES in the moist soil illustrate its eco-friendly biodegradability (Supplementary Fig. 12)[6, 12].

Strain-sensing ability of E-GES

The strain sensing performances of E-GES were verified by attaching them to different body parts (Fig. 4a). As shown in Fig. 4b, the bending degrees of the forefinger are closely associated with the variations

of resistance, and the increase in bending angle lead to an increasing resistance, which can return to the original value when straightening the forefinger. The fixing rotation angle of the wrist generates clear and repeatable resistance signals (Fig. 4c), and large movements of the knee also can be detected by E-GES (Fig. 4d). Furthermore, in order to test the strain sensitivity of E-GES to its limits, we challenge its responsive ability toward the thrust from the breathing. E-GES embedded in a mask can continuously monitor the breathing motion of the volunteer, demonstrating its potential application for real-time health monitoring (Fig. 4e). The slight strain change from the blinking can also be detected by E-GES when attaching it to the middle of the forehead (Fig. 4f). On the other hand, because of its improved gluten network, E-GES can transform the volume change of a balloon into the variation of resistance signals by attaching E-GES to the surface of the balloon. Fig. 4g and 4 h show the increasing and repeatable signals corresponding to the gradually inflating process and the cyclic inflating-deflating process respectively. This means the robust E-GES network exhibits superior sensing abilities even after suffering from three-dimensional spatial changes in strain, a phenomenon currently rarely reported to the best of our knowledge. The E-GES is further examined by the comparison between the work of a E-GES with a notch and that of a normal E-GES (Supplementary Fig. 13). Finally, the stable and recoverable sensing ability of the E-GES network is demonstrated by cyclic stretching-releasing sensing experiments (Fig. 4i).

Conclusion

In summary, we report a new protein (gluten) for fabricating e-skin with stretchability, self-healing ability and biocompatibility. The unique combination of gluten and EGaIn successfully creates a robust gluten network with improved strength and toughness. Moreover, based on the incorporation of EGaIn, the obtained E-GES has an enhanced self-healing ability, and there are no adverse reactions when attaching E-GES to rabbit skin in animal experiments. E-GES not only matches the requirements of an ideal e-skin well, but also demonstrates acute strain sensing ability in different situations, ranging from large-scale human motions to tiny strain changes. This work provides an attractive idea to design e-skin through the construction of protein networks by liquid metal, and this method could be further developed by using other inorganic materials, such as MXene, carbon nanotubes and silver nanofibers, to obtain an e-skin with desired functions.

Methods

General methods. The gluten and EGaIn were purchased from the Meryer (Shanghai) Chemical Technology Co., Ltd. and Shenyang Jiabei Commerce Ltd. respectively. NaCl and methyl cellulose M20 (MC) were obtained from Sinopharm Chemical Reagent Co., Ltd. The above reagents are used without further purification unless otherwise stated. The EGaIn-dispersed solutions were prepared by dispersing different masses of EGaIn in the 1% MC aqueous solution, followed by sonication in an ice bath for 70 min (Supplementary Fig. 14) (Ultrasonic cell disruptor JYD-1800L with a 6-mmφ probe, Shanghai Zhixin Instrument Co., Ltd.). It should be noted that to obtain a robust gluten network, a small amount of NaCl (5.66wt% of the gluten) was firstly dissolved in the 1% MC aqueous solution before the addition of EGaIn.

The E-GES sample was fabricated by mixing equal quality of the EGaIn-dispersed solution and gluten through a hand mixer and kneading (Supplementary Fig. 15). According to the mass ratio of EGaIn to gluten, the obtained four E-GES samples were denoted as 1%, 3%, 5% and 10% respectively, and the control sample was obtained by mixing MC aqueous solution with gluten, which denoted as 0%. The micromorphology of E-GES was observed by field emission scanning electron microscopy (FESEM, Zesis ultra55) equipped with the energy-dispersive X-ray spectroscopy (EDS). Fourier transform infrared spectra (FTIR) were recorded by PROTA-2X^{TM} FT-IR Protein Analyzer and the obtained data was analyzed through GRAMS/AI software. Raman spectroscopy was performed with the Renishaw In Via Qontor confocal Raman microscope that used a 785 nm excitation laser, and the collected Raman spectroscopy data was carried out with WiRE 5.3 software. X-ray photoelectron spectroscopy (XPS) was performed using a Thermo Fisher ESCALAB 250Xi with Al Ka radiation. Differential scanning calorimetry (DSC) was performed on TA Q2000 and samples were heated from 10 °C to 150 °C at 10 °C/min under a nitrogen flow. The free -SH and S-S contents were measured and calculated according to the previous report.[10] The E-GES samples for the above tests were lyophilized before testing, and the following measurements used E-GES samples directly.

Mechanical tests. For mechanical tests, the E-GES samples were shaped by a custom-made cylindrical PTFE mould with an inner diameter of 15 mm and height of 15 mm according to the method of H.C.D. Tuhumury et al[22, 23]. with some modifications. After carefully removing the mould, the shaped samples were glued onto the pneumatic grips and tested with an Instron 5966 tensile tester equipped with a 10 N load cell at a raising rate of 300 mm/min. The mechanical properties of E-GES samples (i.e., the maximum tensile stress, tensile toughness and Young's modulus) were analyzed through the obtained stress-strain curves, and the recovery rate was calculated according to the following formula: stiffness recovery=E_2/E_1´100%, toughness recovery= A_2/A_1´100%, (E_1 and A_1 were the Young's modulus and dissipated energy of the original E-GES, while E_2 and A_2 were the Young's modulus and dissipated energy of the self-healed E-GES).

Rheological tests. The rheological measurements were performed on an Anton Paar Physica MCR 301 rheometer with the 25 mm parallel-plate geometry and a fixed gap of 1 mm at 25 °C. The linear viscoelastic region was obtained by the oscillation measurement with strain values changing from 0.1 % to 1000 % at a constant frequency of 1 Hz, and then the frequency sweeps were carried out in a frequency range of 0.1 Hz to 100 Hz at a fixed strain of 0.5 %.

Biocompatibility tests. For biocompatibility tests, the dorsal areas (about 8 cm^2) of experimental rabbits were partially depilated before testing and a #-shaped wound was introduced into the back of them. The extraction experiment was carried out by immersing E-GES samples in the artificial sweat (by an extraction ratio of 0.1 g:1 mL) at 37 °C for 24h. The E-GES samples were firmly attached to the skin with a #-shaped wound by using the bandage, and treated sweat was dripped in another rabbit skin (Supplementary Fig. 16). These two experiments last for 4h every day. The skin near the experimental

region without any treatments was used as control. These experiments continued for 7 days to evaluate the biocompatibility of E-GES.

Degradation tests. For degradation tests, the pepsin solution was prepared by dissolving 0.3g of pepsin in 30 mL of 0.1 mol/L HCl solution. The degradation tests were carried out by immersing E-GES samples in the obtained pepsin solution and the moist soil respectively at room temperature.

Strain sensing tests. For strain sensing tests, the real-time R-T curves were recorded by a Keithley 2604B SourceMeter instrument.

References

1. Yang JC, Mun J, Kwon SY, Park S, Bao Z, Park S. Electronic Skin: Recent Progress and Future Prospects for Skin-Attachable Devices for Health Monitoring, Robotics, and Prosthetics. *Adv. Mater.* **31**, 1904765 (2019).

2. You I, et al. Artificial multimodal receptors based on ion relaxation dynamics. *Science* **370**, 961-965 (2020).

3. Lee S, et al. Nanomesh pressure sensor for monitoring finger manipulation without sensory interference. *Science* **370**, 966-970 (2020).

4. Jo M, et al. Protein-Based Electronic Skin Akin to Biological Tissues. *ACS Nano* **12**, 5637-5645 (2018).

5. Chen G, et al. Plasticizing Silk Protein for On-Skin Stretchable Electrodes. *Adv. Mater.* **30**, 1800129 (2018).

6. Hou C, et al. A Biodegradable and Stretchable Protein-Based Sensor as Artificial Electronic Skin for Human Motion Detection. *Small* **15**, 1805084 (2019).

7. Wang Q, Jian M, Wang C, Zhang Y. Carbonized Silk Nanofiber Membrane for Transparent and Sensitive Electronic Skin. *Adv. Funct. Mater.* **27**, 1605657 (2017).

8. Wang Q, Ling S, Liang X, Wang H, Lu H, Zhang Y. Self-Healable Multifunctional Electronic Tattoos Based on Silk and Graphene. *Adv. Funct. Mater.* **29**, 1808695 (2019).

9. Du J, Dang M, Khalifa I, Du X, Xu Y, Li C. Persimmon tannin changes the properties and the morphology of wheat gluten by altering the cross-linking, and the secondary structure in a dose-dependent manner. *Food Res. Int.* **137**, 109536 (2020).

10. Liu R, Shi C, Song Y, Wu T, Zhang M. Impact of oligomeric procyanidins on wheat gluten microstructure and physicochemical properties. *Food Chem.* **260**, 37-43 (2018).

11. Lei Z, Huang J, Wu P. Traditional Dough in the Era of Internet of Things: Edible, Renewable, and Reconfigurable Skin-Like Iontronics. *Adv. Funct. Mater.* **30**, 1908018 (2019).

12. Hu M, et al. A flour-based one-stop supercapacitor with intrinsic self-healability and stretchability after self-healing and biodegradability. *Energy Storage Mater.* **21**, 174-179 (2019).

13. Kang J, et al. Tough and Water-Insensitive Self-Healing Elastomer for Robust Electronic Skin. *Adv. Mater.* **30**, 1706846 (2018).

14. Zhang Q, Shi C-Y, Qu D-H, Long Y-T, Feringa BL, Tian H. Exploring a naturally tailored small molecule for stretchable, self-healing, and adhesive supramolecular polymers. *Sci. Adv.* **4**, eaat8192 (2018).

15. Li CH, et al. A highly stretchable autonomous self-healing elastomer. *Nat. Chem.* **8**, 618-624 (2016).

16. Yu Y, Miyako E. Manipulation of Biomolecule-Modified Liquid-Metal Blobs. *Angew. Chem., Int. Ed. Engl.* **56**, 13606-13611 (2017).

17. Yamaguchi A, Mashima Y, Iyoda T. Reversible Size Control of Liquid-Metal Nanoparticles under Ultrasonication. *Angew. Chem., Int. Ed. Engl.* **54**, 13000 –13004 (2015).

18. Fang G, Tang Y, Qi Z, Yao J, Shao Z, Chen X. Precise correlation of macroscopic mechanical properties and microscopic structures of animal silks-using Antheraea pernyi silkworm silk as an example. *J. Mater. Chem. B* **5**, 6042-6048 (2017).

19. Balu R, et al. Tough Photocrosslinked Silk Fibroin/Graphene Oxide Nanocomposite Hydrogels. *Langmuir* **34**, 9238-9251 (2018).

20. Wang K, et al. Effects of partial hydrolysis and subsequent cross-linking on wheat gluten physicochemical properties and structure. *Food Chem.* **197**, 168-174 (2016).

21. Tuhumury HCD, Small DM, Day L. The effect of sodium chloride on gluten network formation and rheology. *J. Cereal Sci.* **60**, 229-237 (2014).

22. Tuhumury HC, Small DM, Day L. Effects of Hofmeister salt series on gluten network formation: Part I. Cation series. *Food Chem.* **212**, 789-797 (2016).

23. Tuhumury HC, Small DM, Day L. Effects of Hofmeister salt series on gluten network formation: Part II. Anion series. *Food Chem.* **212**, 798-806 (2016).

24. Nawrocka A, Szymańska-Chargot M, Miś A, Wilczewska AZ, Markiewicz KH. Effect of dietary fibre polysaccharides on structure and thermal properties of gluten proteins – A study on gluten dough with application of FT-Raman spectroscopy, TGA and DSC. *Food Hydrocolloids* **69**, 410-421 (2017).

25. Bazylewski P, Divigalpitiya R, Fanchini G. In situ Raman spectroscopy distinguishes between reversible and irreversible thiol modifications in l-cysteine. *RSC Adv.* **7**, 2964-2970 (2017).

26. Lu Y, et al. Controlling Defects in Continuous 2D GaS Films for High-Performance Wavelength-Tunable UV-Discriminating Photodetectors. *Adv. Mater.* **32**, 1906958 (2020).

27. Lim HR, Kim HS, Qazi R, Kwon YT, Jeong JW, Yeo WH. Advanced Soft Materials, Sensor Integrations, and Applications of Wearable Flexible Hybrid Electronics in Healthcare, Energy, and Environment. *Adv. Mater.* **32**, 1901924 (2019).

28. Huang J, et al. Stretchable and Heat-Resistant Protein-Based Electronic Skin for Human Thermoregulation. *Adv. Funct. Mater.* **30**, 1910547 (2020).

29. Cao Y, et al. Self-healing electronic skins for aquatic environments. *Nat. Electron.* **2**, 75-82 (2019).

30. Zhang LM, et al. Self-Healing, Adhesive, and Highly Stretchable Ionogel as a Strain Sensor for Extremely Large Deformation. *Small* **15**, 1804651 (2019).

31. Darabi MA, et al. Skin-Inspired Multifunctional Autonomic-Intrinsic Conductive Self-Healing Hydrogels with Pressure Sensitivity, Stretchability, and 3D Printability. *Adv. Mater.* **29**, 1700533 (2017).

32. Su D, Yao M, Liu J, Zhong Y, Chen X, Shao Z. Enhancing Mechanical Properties of Silk Fibroin Hydrogel through Restricting the Growth of beta-Sheet Domains. *ACS Appl. Mater. Interfaces* **9**, 17489-17498 (2017).

33. Cera L, et al. A bioinspired and hierarchically structured shape-memory material. *Nat. Mater.* **20**, 242-249 (2021).

34. Rygula A, Majzner K, Marzec KM, Kaczor A, Pilarczyk M, Baranska M. Raman spectroscopy of proteins: a review. *J. Raman Spectrosc.* **44**, 1061-1076 (2013).

35. Zhu Y, Wang Y, Li J, Li F, Teng C, Li X. Effects of Water-Extractable Arabinoxylan on the Physicochemical Properties and Structure of Wheat Gluten by Thermal Treatment. *J. Agric. Food Chem.* **65**, 4728-4735 (2017).

Declarations

Author information

These authors contributed equally: Yudong Cao, Bin Chen.

These authors jointly supervised this work: Mingxin Ye, Jianfeng Shen.

Affiliations

Institute of Special Materials and Technology, Fudan University, Shanghai, China

Bin Chen, Yudong Cao, Ziyi Cao, Wei Yao, Mingxin Ye & Jianfeng Shen

State Key Laboratory of Molecular Engineering of Polymers, Department of Macromolecular Science, Fudan University, Shanghai, China

Zhuo Yan, Yixiu Qin & Chang Sun

State Key Laboratory of Food Nutrition and Safety, Tianjin University of Science & Technology, Tianjin, China

Rui Liu & Yunjiao Zhao

Department of Chemistry, Fudan University, Shanghai, China

Bin Chen, Yudong Cao, Ziyi Cao & Minying Wu

Department of Mechanical Engineering, George Mason University, VA, USA

Pei Dong & Mason Oliver Lam Chee

Department of Materials Science and NanoEngineering, Rice University, Houston, TX, USA

Xiang Zhang and Pulickel M. Ajayan

RENISHAW (Shanghai) Trading CO.LTD, SPD, Shanghai, China

Zhaofen Li

Contributions

Bin Chen and Yudong Cao conceived and designed the work, prepared E-GES, conducted sensing experiments and contributed to manuscript writing. Zhuo Yan, Minying Wu and Yixiu Qin performed the rheological measurements, DSC, SEM and analyzed related data. Rui Liu and Yunjiao Zhao conducted -SH and S-S contents tests, related data analysis and contributed to the interpretation of cross-linking mechanism. Ziyi Cao, Wei Yao, Chang Sun and Zhaofen Li conducted the Raman spectroscopy, FTIR spectroscopy, analyzed related data and interpreted the secondary structure reconfiguration of gluten. Mingxin Ye and Jianfeng Shen performed tensile experiments and funded this work. Pei Dong, Mason Oliver Lam Chee, Xiang Zhang and Pulickel M. Ajayan edited the manuscript and took part in the discussion of results.

Corresponding authors

Correspondence to Mingxin Ye or Jianfeng Shen.

Ethics declarations

Competing interests

The authors declare no competing interests.

Ethics statement

The volunteers (Yudong Cao and Bin Chen) agreed to all strain-sensing experiments in this manuscript with informed consent.

Animal studies

All institutional and national guidelines for the care and use of laboratory animals were followed in animal experiments.

Figures

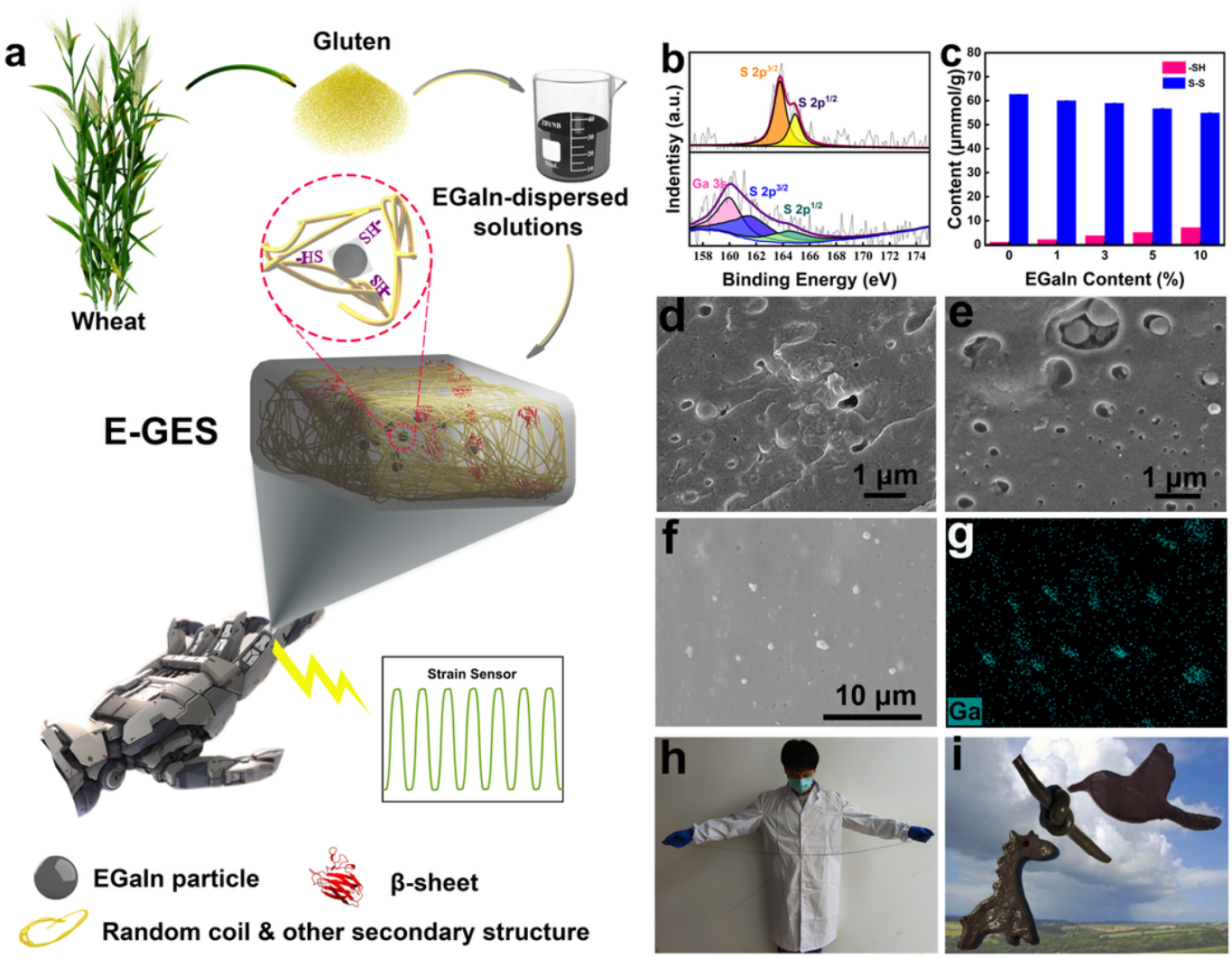

Figure 1

Schematic drawings of preparing E-GES and the analysis of relevant chemical bonds as well as the morphology of E-GES. a, Schematic illustration of the fabrication process of E-GES. b, The X-ray photoelectron spectroscopy (XPS) of the control sample (the top) and the 5% E-GES (the bottom). For the control sample, the S 2p region show the S 2p3/2 and S 2p1/2 components at the binding energies of 163.8 eV and 164.9 eV respectively, while these two peaks in the 5% E-GES sample show shifts toward the low binding energies direction, appearing at 161.6 eV and 164.5 eV respectively. This means the formation of EGaln-SH coordinative bonds in E-GES, consistent with the previous reports16, 26. c, The -SH and S-S content of different E-GES samples. d, e, SEM micrograph of the control sample (d) and the 5% E-GES sample (e). f, g, SEM micrograph of 5% E-GES sample (f) and the corresponding EDS element mapping micrograph (g). h, Photograph of the stretched E-GES sample. The 5% E-GES can be stretched out easily for more than 10 times. i, Photograph of E-GES with different shapes. The E-GES can be molded to different complex shapes, i.e., knot, bird and giraffe.

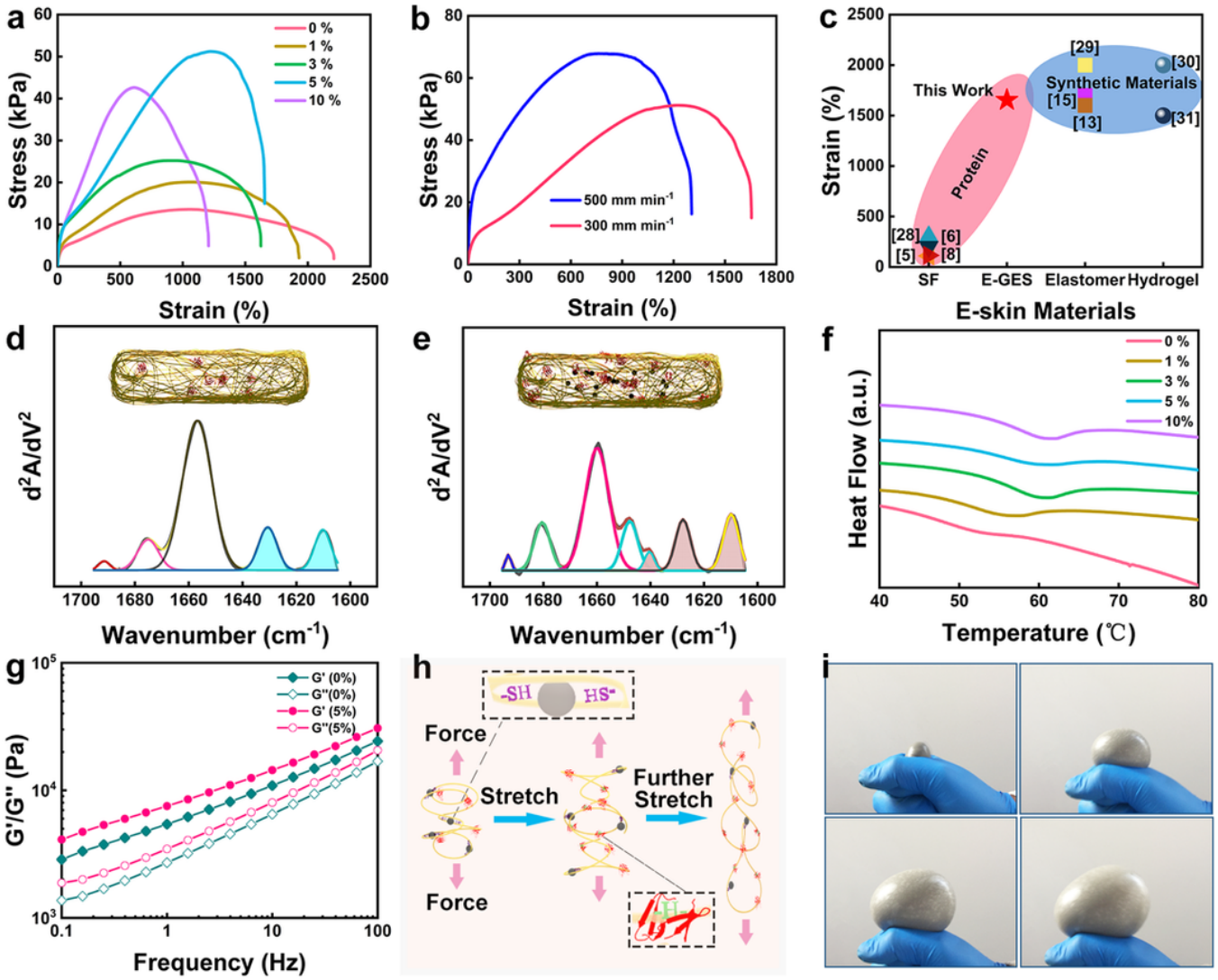

Figure 2

Characterization of the macroscopic mechanical properties and the microscopic structures of E-GES. a, Stress-strain curves of different E-GES samples. b, Stress-strain curves of 5% E-GES at different strain rates. The E-GES can resist the increasing strain rate without showing brittleness fracture, and exhibits a rising tensile toughness, meaning the breakage of more dynamic chemical bonds in the tough E-GES network to dissipate energy when applying a high tensile rate. c, Maximum tensile strain comparison between protein-based e-skins and synthetic material-based e-skins. d, e, The calculated secondary structure results of the control sample (d) and 5% E-GES (e) from the analysis of the amide I band in their FTIR spectra (Supplementary Fig. 1). The peaks within the range of 1610-1640 cm-1 are attributed to β-sheets, filled with blue (d) and brown (e) color respectively. Inset: The content of the β-sheets and EGaIn in the E-GES network. f, DSC thermogram of different E-GES samples. g, Frequency sweep curves of G' and G" for the control sample and 5% E-GES. h, Schematic illustration the stretching process of E-GES. The presence of EGaIn-SH coordinative bonds and the intermolecular H-bonds of β-sheets are in favor of

energy dissipation. i, Photographs of the inflation process of E-GES. The E-GES can be sealed on the inflation port (port diameter 1cm) of the air pump, and then be inflated into a big balloon.

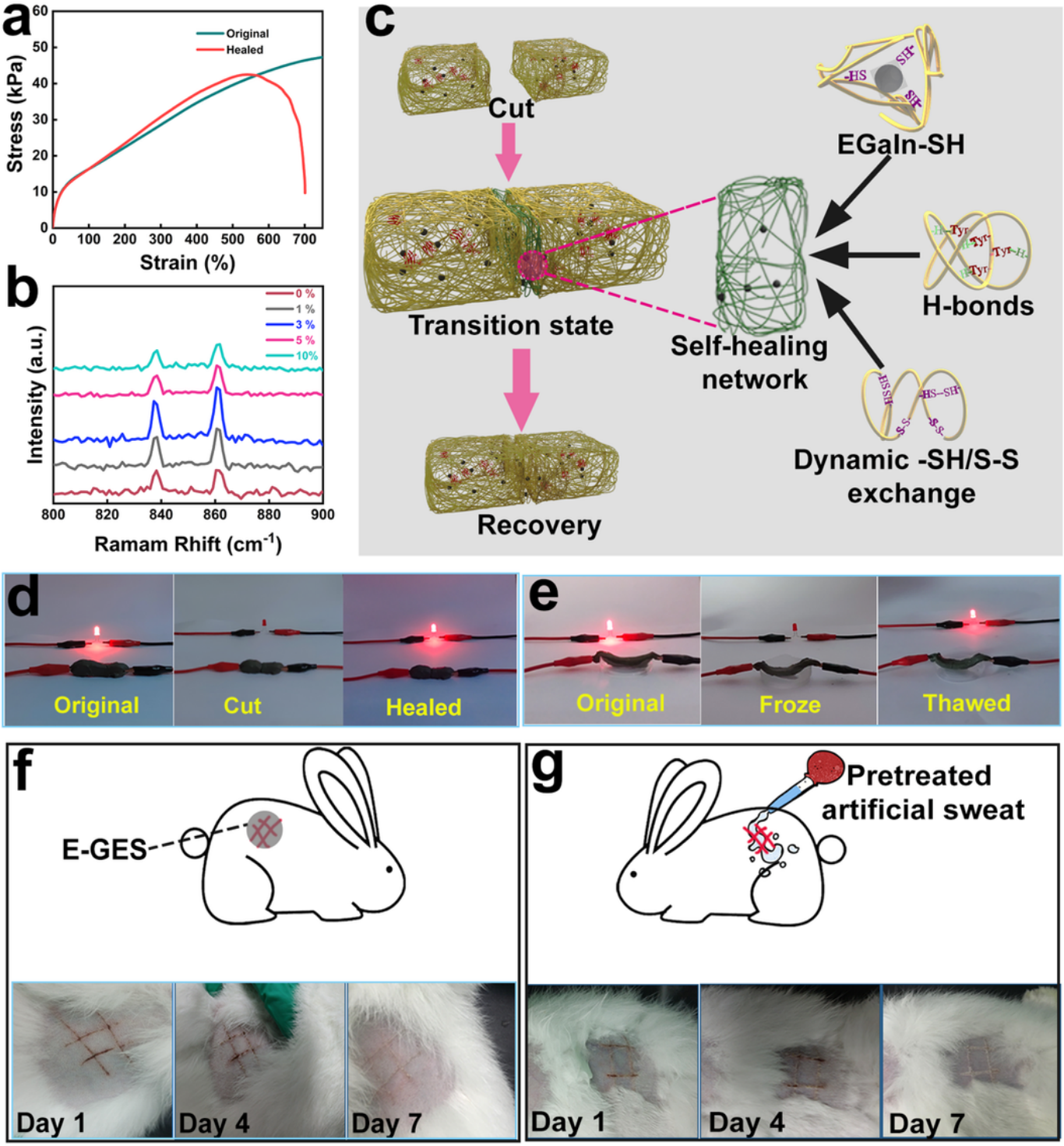

Figure 3

Characterization of the self-healing ability and biocompatibility of E-GES. a, Stress-strain curves of pristine (green) and self-healed (red) 5% E-GES samples. In the self-healing process, two fresh cut-off E-GES pieces are allowed to simply contact together without using other assistance methods, and the re-

shaped E-GES recovers almost its original Young’s modulus in 1 min. b, Raman spectra of different E-GES samples. The Tyr doublet peaks appear at 861 cm-1 and 837 cm-1 respectively. c, Schematic illustration of the proposed self-healing mechanism of E-GES network. The green E-GES network represents a self-healing transition state, arising from the formation of various dynamic chemical bonds, including EGaIn-SH coordinative bonds, noncovalent H-bons and dynamic S-S covalent bonds, in contacting cut-interfaces. d, e, Photographs of E-GES connected with a LED bulb in different situations. There is the liquid nitrogen in the plastic container (e). f, g, Photographs of biocompatibility experiments of E-GES on the rabbit skin. The skin is treated by E-GES (f) and pretreated artificial sweat (h) respectively. The pretreated artificial sweat was prepared by immersing E-GES into the artificial sweat for 24h.

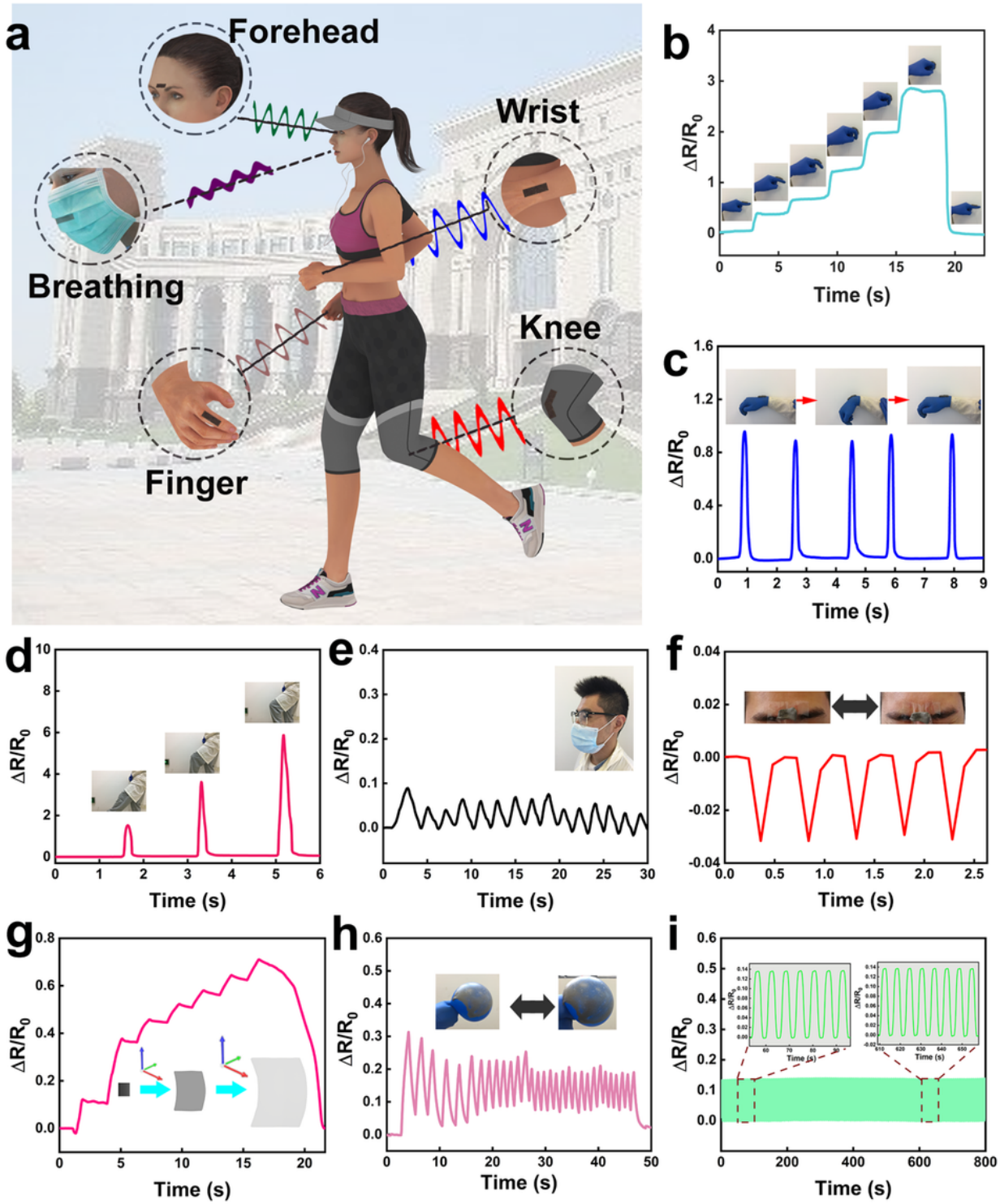

Figure 4

Characterization of the strain-sensing ability of E-GES. a, Schematic illustration of strain-sensing tests on different body parts. b, c, d, Real-time resistance changes of E-GES when being adhered to the forefinger (b), the wrist (c) and the knee (d). Inset, photographs of the bending process of the forefinger (b), the wrist (c) and the knee (d). e, Real-time resistance changes of E-GES when being embedded in a mask. E-GES can detect the minor strain changes from the breathing. f, Real-time resistance changes of E-GES when

being adhered to the middle of the forehead. E-GES can monitor deformations of facial expressions. g, h, Real-time resistance changes of E-GES when being adhered to the surface of the balloon. Inset, schematic illustration of the increasing strain change of E-GES in the three-dimensional direction (g) and photographs of E-GES on the surface of the balloon surface (h). i, Stability tests of E-GES under stretch at 50% for more than 100 cycles.

Supplementary Files

This is a list of supplementary files associated with this preprint. Click to download.

- Supplementaryinformation.docx